Phantom Study: Area and Clarity of Myocardial Wall Non-per Fused Defect Acquired using SPECT

Mohannad Adel Sayah[1*], Norlaili Ahmad Kabir[2], Mohamad Suhaimi Jaafar[3]

[1]School of physics, Universiti Sains Malaysia
11800USM, Penang, Malaysia

[2]School of physics, Universiti Sains Malaysia
11800USM, Penang, Malaysia

[3]School of physics, Universiti Sains Malaysia
11800USM, Penang, Malaysia

[*]*Corresponding author's email: moh77_sayah [AT] yahoo.com*

ABSTRACT---- ***Physician's interpretation worked continuously to improve nuclear image to be of perfect quality. Single photon emission computed tomography (SPECT) is one of the most important methods to assess the diagnosis of diseases. Myocardial perfusion imaging (MPI) studies consider the accuracy of defect area is most important to estimate precisely the severity of the infraction. The defect area inside myocardial wall defined as the coldest spot in SPECT images where the blood does not per-fused through this spot. In our study we used fabricated phantom from polyethylene plastic consist of two chambers to simulate myocardial wall of the left ventricle in end-diastole and end-systole. 4 plastic defects in same thickness were inserted at 4 regions inside myocardial phantom. Clarity of the defect of acquired SPECT images is defined by thickness. Our work was carried out to measure the defect area of SPECT myocardial image with depending on the positioning of phantom on an imaging table. The results showed that clarity of defect of acquired SPECT depends on location of the defect related to myocardial thickness (end-diastole, end-systole), and on positioning of the phantom. The measured area of the defect in acquired SPECT image was compared with true defect area. The measured defect area in SPECT images in comparison with true defect area has varied results depending on the thickness of myocardial wall phantom(end-diastole, end-systole) and on the positioning of the phantom as follows: underestimated 6% and 4% at the centre for end-diastole and end-systole respectively, and overestimation 2%, 5%, 9% and 1%, 3%, 6% at off-centre for end-diastole and end-systole respectively that when the myocardial phantom positioned at 5 cm, 10 cm, and 15 cm on an imaging table.***

Keywords---- Clarity. Defect area. Myocardial wall. Positioning. SPECT

---

1. INTRODUCTION

Cardiovascular diseases remain the biggest cause of death worldwide[1]. Single photon emission computed tomography (SPECT) is the most widely used test for the assessment of myocardial diseases [2]. Many SPECT perfusion studies were focused to determine the defect size and severity [3-5]. Author [6] in his perfusion SPECT study explained there is less 2% error of defect size comparison to true size. Author [7] used seven defects in varying size to estimate the accuracy of defect size with mean± standard deviation. Author [3] reported absolute error increasing when true defect size decreased 8% for large defects and 37% of the small defect size. (SPECT) imaging to be in best case the patient position should be on the appropriate with imaging table to correspond with the infected organ below rotation of gamma heads camera [6]. Several studies in nuclear SPECT imaging focused on appropriate patient body position on an imaging table with the gamma camera rotation [9, 10]. SPECT clinical studies consider the measuring area of defect size in myocardial wall is very important to give an accurate diagnosis of disease [11, 12]. Quality of cardiac perfusion SPECT methods needs external quality control test [13].

Tissue in the myocardial wall requires its own constant supply of oxygen and nutrients by blood, when blood blocked the tissue become starved, and then causing the death of tissue [14]. In myocardial perfusion study, the healthy tissue is rich of blood, but starved tissue has less blood. In similar, in SPECT image of myocardial wall the area of healthy tissue has maximum uptake counts (hot spot), but in non healthy tissue (starved and dead) the area has less up taking or haven't

(cold spot). The clarity and the area for the defect of myocardial SPECT image are very important to diagnose the severity of disease. Clarity and area of the defect in SPECT image have relationship with factors such as: defect location within myocardial wall, and thickness of the defect. Hence, the purpose of our study was to show that defect clarity and defect area of SPECT myocardial image depend on the positioning of the phantom on an imaging table.

2. MATERIAL AND METHOD

2.1 Phantom configuration

Hollow cylindrical phantom were fabricated to simulate heart in two configurations, end-diastole and end-systole. The phantom material is made of polyethylene plastic (number of electron per gram = 0.57, density = 0.93 g/cm^3) [15] was used in this study (Figure 1). The atomic number and density of the phantom material were corresponding to the atomic number and density of myocardial wall muscle (number of electron per gram = 0.55, density= 1 g/cm^3). The phantom consisted of two hollow chambers. A hollow inner chamber (5 cm in diameter, 8.5 cm in length) for End-diastole, and (3.6 cm in diameter, 7.4 cm in length) for End-systole. The inner chamber placed inside a large hollow outer chamber. The measurements of the outer chamber were (7.2 cm in diameter, 9.6 cm in length) for the End-diastole, and (6 cm in diameter, 8.6 cm in length) for End-systole. The volume of space between two chambers was 175 ml for End-diastole and 125 ml for End-systole. The width of a space between two chambers for end-diastole and end-systole is (11 mm, 12 mm) respectively. The space was created to simulate the myocardial wall of the left ventricle. The hollow inner chamber was filled thoroughly with water. 4 polyethylene plastic cubes defined as defects were inserted on the outer surface of the inner chamber. The defects were fixed by commonly glue worked well in water. The dimensions of defects in (mm unit) are (20x20) on locations, basel, mid, and apex. The defects fixed in basel, mid, and apex separately. For area of defect test we used only 5 mm thickness on mid location. These defects were located at commonly four regions of myocardial wall: anterior, septal, inferior and lateral. For (SPECT) phantom of myocardial wall of left ventricle the space between two chambers was filled of technetium-99m (Tc-99m) solution with water in concentration 0.0925 MBq/ml calculated as basis average of myocardial wall uptake 1% of patient dose [16]. In this study, the phantom had been placed in plastic container (20 cm x 20 cm) filled with Tc-99m solution mixed with 2 liters of water. We were not taken into account the affection of attenuation, scattering, motion, respiratory and the organs like lungs and spins, because we believe the reasons which estimate the artifacts are not considered in all clinical studies.

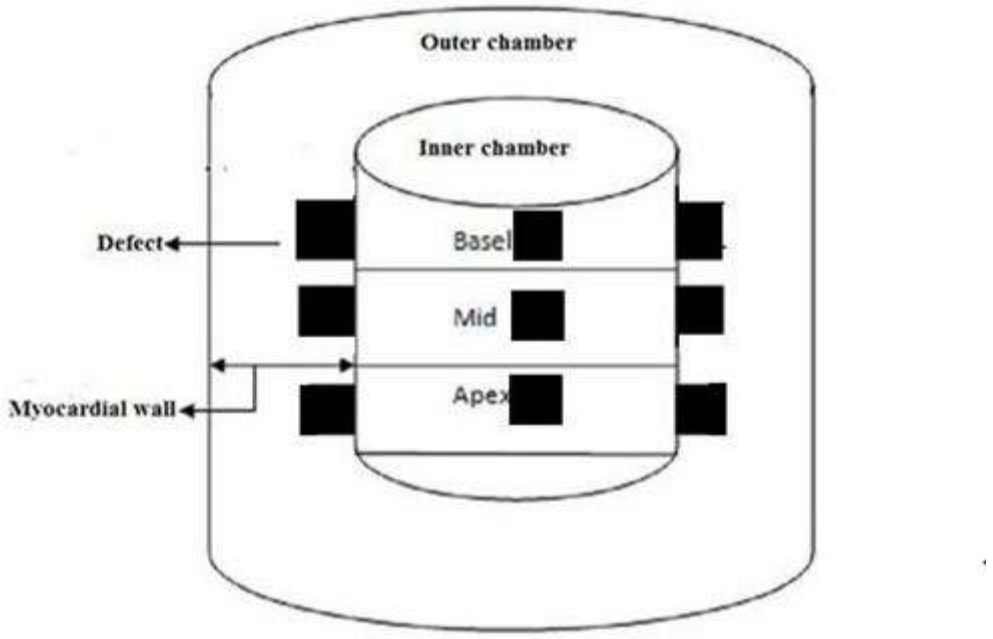

Figure 1: Schematic phantom to simulate myocardial wall of left ventricle with 4 plastic cubs (defect) in same dimensions (20x20) (mm) located in 3 regions within myocardial phantom (basel, mid, and apex). The plastic cubs fixed on the outer surface of inner chamber

2.2 Image acquisition

Dual-head gamma camera low-energy high (Discovery NM/CT670 Pro), parallel hole collimator. Tc-99m (140) Kev energy window is 20%. A 180° circular orbit, 25 cm orbit radius. The imaging was performed using step-and- shot protocol 60 projections 3° for each projection, 20 seconds per projection. The total acquisition time 10 minutes for two head gamma camera. The matrix size is 64X64. All images were acquired in two long axes (vertical and horizontal) and reconstructed by Butterworth filter (order 10, 0.5 cut-off frequency), and the images were stored in DICOM format. The phantom was angled 26° with imaging table to simulate a real heart. The centerline of heads gamma camera was symmetric with mid of phantom. The adjacent camera heads were moved (180°), 135° degree of posterior until -45° anterior. The images were acquired at 4 phantom positions on the imaging table, 5cm, 10cm and 15cm (Figure 2). The area of defects was specified by the presence of average pixels with mean value less than 50% of intensity in comparison to the maximum mean pixel for other non- defects area. The area of defects was reported as (mean of area) in mm^2 unit from 14 image slices that were acquired. The defect area performed using software free image j 1.48v.

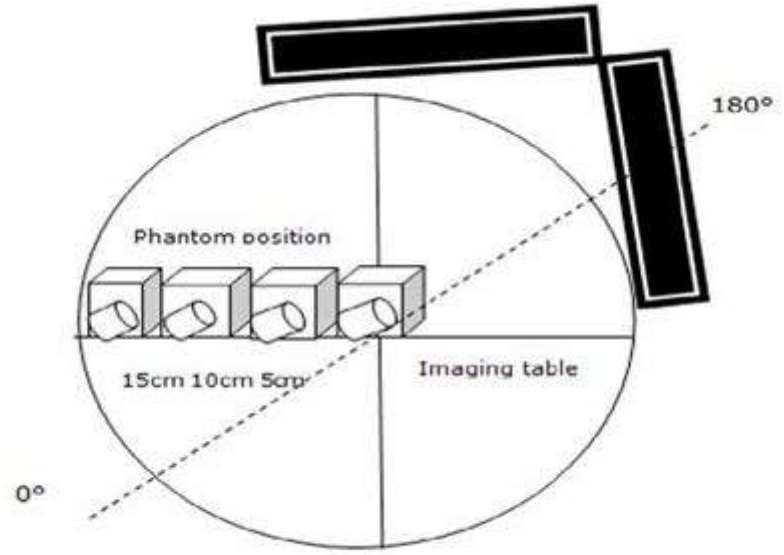

Figure 2: Schematics of 4 myocardial phantom positions included the centre with 180° acquisition from -45° posterior to 135° anterior

3. RESULTS AND DISSCUSION

3.1 Clarity of the defect in SPECT myocardial image.

Center position, results showed the clarity (thickness detected) of the defect in SPECT myocardial image depends on the location of the defect within myocardial phantom. Clarity of the defects of all regions of SPECT myocardial image (anterior, septal, inferior, and lateral) was achieved at 4mm in mid, 5 mm in apex, and 6 mm in basel. Perhaps the loss of the Tc-99m counts in apex and basel regions related to many physics factors such as: photon scatter, and its attenuation. . Maybe positioning of the phantom contributes as a part of artifacts, and this causes negative effects on clarity of defects. The artifacts of enhanced contrast and geometric distortion are caused by depth depend spatial resolution [17].

Off-center position, the affection of positioning of the phantom on the defect clarity of all regions (anterior, septal, inferior, and lateral) of SPECT myocardial images was investigated (Figure 3, 4). When the myocardial phantom was positioned at 15 cm off-centre of imaging table, the results showed that in end-diastole the defects appeared clearly of all regions at 3 mm in mid, and 4 mm in apex and basel, whereas 4 mm thickness seen clearly in 3 regions in end-systole. Although the defect in mid location has 3 mm thickness less than its in basel location 4 mm, but the clarity of defect was better particularly, when the phantom positioned at 15 cm off-centre of imaging table.

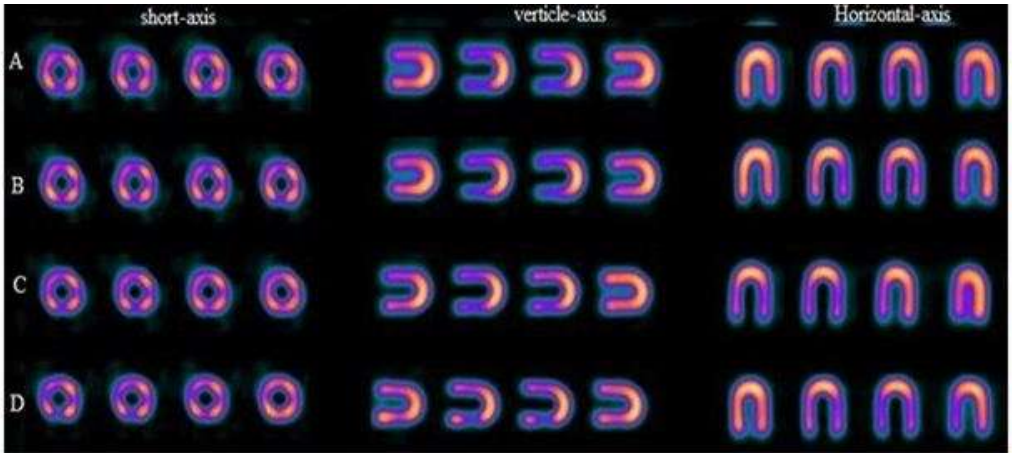

Figure 3: SPECT short-axis and long axis slices (verticle, horizontal), when 3 mm thickness of defect located in mid region of myocardial phantom (end-diastole). The defect appeard in 4 loctions (anterior, septal, inferior, and latera).Row(A) at the center, and rows (B, C, and D) off- center, where row(B) at 5 cm , row(C) at the 10 cm, and row (D) at 15 cm

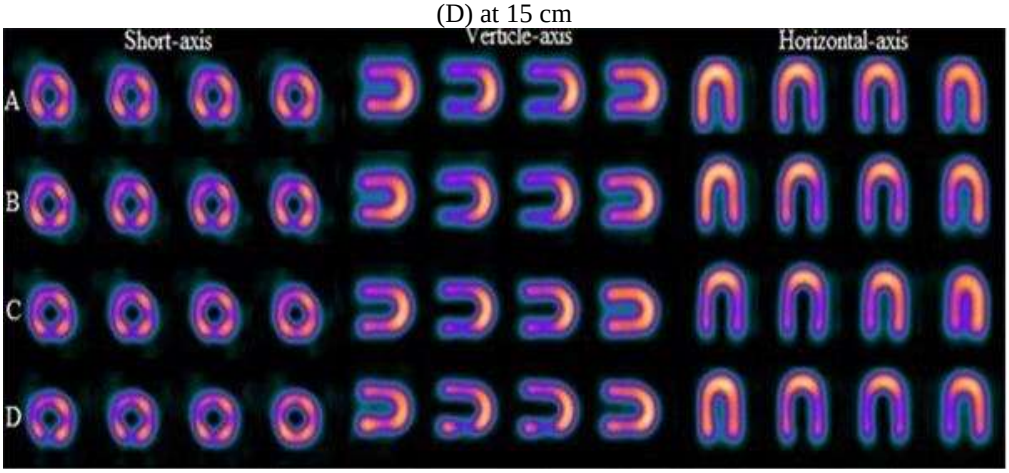

Figure 4: SPECT short-axis and long axis slices (verticle, horizontal), when 4mm thickness of defect located in basel region of myocardial phantom (end-systole). The defect appeard in 4 loctions (anterior, septal, inferior, and latera).Row(A) at the center, and rows (B, C, and D) off- center, where row(B) at 5 cm , row(C) at the 10 cm, and row (D) at 15 cm

3.2 defects Area

End-diastole phantom, in SPECT myocardial images the mean area for the defect and myocardial wall in comparison with true area, the results showed a variety of the percentage of the area depending on positioning for the phantom on an imaging table (Table 1). Results showed the percentage of the SPECT defect area to true defect area increases ascending with eccentric of the position of the phantom: (94%, 101%, 103%, and 106%) at the center, 5 cm, 10 cm, and 15 cm respectively. In similar, the percentage of SPECT defect area to true myocardial area was increased with eccentric position of the phantom: (17.9%, 19%, 19.5%, and 20%).

Table 1: Value and percentage of mean area for the defect and the myocardial wall in SPECT image, when the end-diastole phantom positioned at 4 positions on an imaging table

position	SPECT area of MW Mean(mm^2)	SPECT area of MW/ True area of MW %	SPECT area of defect Mean(mm^2)	SPECT area of defect/true area of defect %	SPECT area of defect/true area of MW %
A	2042	97	376	94	17.9
B	2127	101	404	101	19.0
C	2169	103	412	103	19.5
D	2253	107	424	106	20.0

MW: myocardial wall, %: percentage, A at the center, B at 5 cm, C at 10 cm, and D at 15 cm

End-systole phantom, when the phantom was positioned off-centre, SPECT image showed a variety of SPECT area for myocardial wall and the defect. This a variety of mean area became increasingly apparent with eccentric position of the phantom in both areas of myocardial wall and defect (Table 2).

Table 2: Value and percentage of mean area for the defect and the myocardial wall in SPECT image, when the end-systole phantom positioned at 4 positions on an imaging table

position	SPECT area of MW Mean(mm^2)	SPECT area of MW/ True area of MW %	SPECT area of defect Mean(mm^2)	SPECT area of defect/true area of defect %	SPECT area of defect/true area of MW %
A	1778	98	392	96	21.7
B	1880	104	416	102	23.0
C	1916	106	424	105	23.5
D	1989	110	440	109	24.3

MW: myocardial wall, %: percentage, A at the center, B at 5 cm, C at 10 cm, and D at 15 cm

The results demonstrated percentage of defect area of SPECT image was convergent at the center of imaging table, when the SPECT defect area was compared with true myocardial area and true defect area, while this percentage divergent gradually with the increased phantom position (Figure 5, 6).

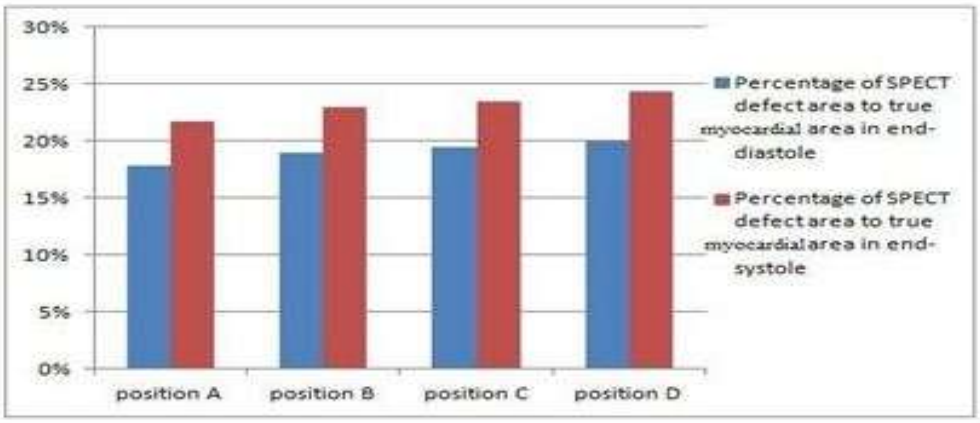

Figure 5: Percentage of SPECT defect area to true myocardial area in end-diastole and end-systole, when the phantom positioned at 4 positions, (A) at the center, (B, C, and D) at off- center, where (B) at 5 cm, (C) at 10 cm, and (D) at 15 cm

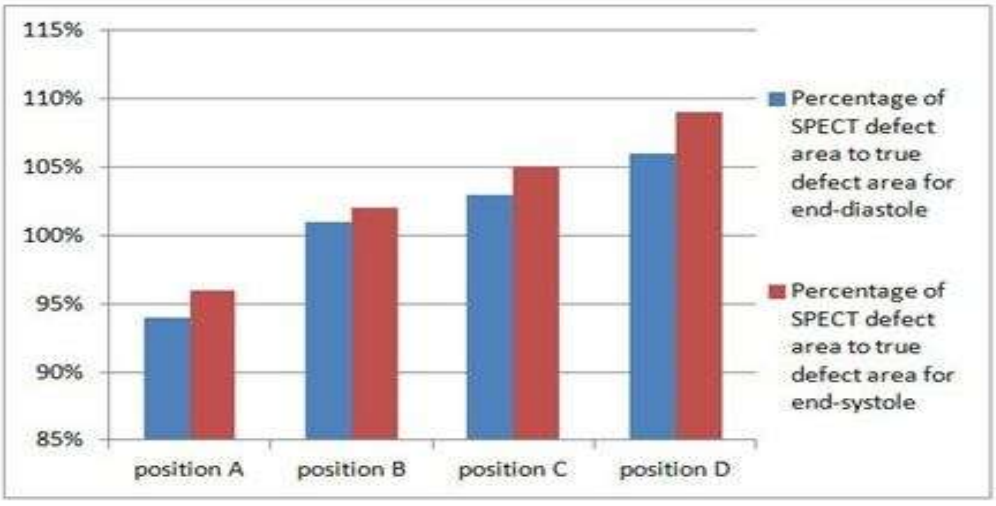

Figure 6: Percentage of SPECT defect area to true defect area in end-diastole and end-systole, when the phantom positioned at 4 positions, (A) at the center, (B, C, and D) at off- center, where (B) at 5 cm, (C) at 10 cm, and (D) at 15 cm

At center position, Quantitatively, SPECT slightly underestimated defect and myocardial area when the phantom was positioned at the center. This underestimated accrued whether the phantom configuration was end-diastole or end-systole. In addition, this underestimated was in less degree in end-diastole than in end-systole.

In our study, the fabricated phantom with inserted defects showed by acquiring SPECT images, that is defect area depend on location within myocardial wall and on the phantom position. The SPECT defect area was decreased at the centre position in comparison with true defects, because degradation of spatial resolution was accrued. This finding agrees with the previous studies of defect size [18]. In SPECT imaging, when the phantom was not on the centre (off-centre of imaging table) the circular radius of two heads camera is not equal at each projection. The circular motion of gamma detector have different displacement, this maybe explain the increasing of defect area whenever increases the distance of phantom from the centre of imaging table. In addition, the defect location has relation with the positions of phantom, where which it was very close to gamma detector heads are better evaluated in comparison with not closed.

4. CONCLUSION

The defect of myocardial SPECT image has differential of the clarity related to myocardial thickness of phantom (diastole, systole), and correlated with position of the phantom on an imaging table. The defect area of myocardial SPECT image has relation with the positioning and thickness of the myocardial phantom on an imaging table, this push to take into account the determination of the best position of the organs for performing the quality center (QC) procedure.

5. REFERENES

[1] Mendis S, Puska P, Norrving B. Global atlas on cardiovascular disease prevention and control: World Health Organization; 2011.

[2] Greenwood JP, Maredia N, Younger JF, Brown JM, Nixon J, Everett CC, et al. Cardiovascular magnetic resonance and single-photon emission computed tomography for diagnosis of coronary heart disease (CE-MARC): a prospective trial. The Lancet. 2012;379(9814):453-60.

[3] Berman DS, Kang X, Slomka PJ, Gerlach J, de Yang L, Hayes SW, et al. Underestimation of extent of ischemia by gated SPECT myocardial perfusion imaging in patients with left main coronary artery disease. Journal of Nuclear Cardiology. 2007;14(4):521-8.

[4] Mahmarian JJ, Cerqueira MD, Iskandrian AE, Bateman TM, Thomas GS, Hendel RC, et al. Regadenoson induces comparable left ventricular perfusion defects as adenosine: a quantitative analysis from the ADVANCE MPI 2 trial. JACC: Cardiovascular Imaging. 2009;2(8):959-68.

[5] Berti V, Sciagrà R, Acampa W, Ricci F, Cerisano G, Gallicchio R, et al. Relationship between infarct size and severity measured by gated SPECT and long-term left ventricular remodelling after acute myocardial infarction. European Journal of Nuclear Medicine and Molecular Imaging. 2011;38(6):1124-31.

[6] Gibbons RJ. Assessment of infarct size and severity by quantitative myocardial SPECT: results from a multicenter study using a cardiac phantom. The Journal of Nuclear Medicine. 2000;41(8):1383.

[7] Benoit T, Vivegnis D, Foulon J, Rigo P. Quantitative evaluation of myocardial single-photon emission tomographic imaging: application to the measurement of perfusion defect size and severity. European Journal of Nuclear Medicine and Molecular Imaging. 1996;23(12):1603-12.

[8] Movahed A, Gnanasegaran G, Buscombe J, Hall M. Integrating Cardiology for Nuclear Medicine Physicians. Alemanha: Springer Verlag. 2009.

[9] Cullom S, Case J, Bateman T. Attenuation correction in myocardial perfusion SPECT. Cardiac SPECT imaging 2nd ed Philadelphia: Lippincott Williams & Wilkins. 2001:89-102.

[10] Zeng GL, Christian PE. Easy Method of Patient Positioning for Convergent-Beam Cardiac SPECT. Journal of nuclear medicine technology. 2007;35(3):131-4.

[11] Sharma P, Patel CD, Karunanithi S, Maharjan S, Malhotra A. Comparative Accuracy of CT Attenuation-Corrected and Non–Attenuation-Corrected SPECT Myocardial Perfusion Imaging. Clinical nuclear medicine. 2012;37(4):332-8.

[12] Lyra M, Sotiropoulos M, Lagopati N, Gavrilleli M, editors. Quantification of myocardial perfusion in 3D SPECT images-stress/rest volume differences. Imaging Systems and Techniques (IST), 2010 IEEE International Conference on; 2010: IEEE.

[13] Heikkinen J, Ahonen A, Kuikka JT, Rautio P. Quality of myocardial perfusion single-photon emission tomography imaging: multicentre evaluation with a cardiac phantom. European journal of nuclear medicine. 1999;26(10):1289-97.

[14] Katz MJ, Ness SM. Coronary Artery Disease (CAD). 2015.

[15] Hubbell JH, Seltzer SM. Tables of X-ray mass attenuation coefficients and mass energy-absorption coefficients 1 keV to 20 MeV for elements Z= 1 to 92 and 48 additional substances of dosimetric interest. National Inst. of Standards and Technology-PL, Gaithersburg, MD (United States). Ionizing Radiation Div., 1995.

[16] Vallejo E. New radiotracers in cardiac imaging: Principles and applications taillefer and Tamaki. Journal of Nuclear Cardiology. 1999;6(5):549-50.

[17] Knesaurek K, King MA, Glick SJ, Penney BC. Investigation of causes of geometric distortion in 180 degrees and 360 degrees angular sampling in SPECT. Journal of nuclear medicine: official publication, Society of Nuclear Medicine. 1989;30(10):1666-75.

[18] Kirac S, Franc J, Liu Y-H. Validation of the Yale circumferential quantification method using (201) T1 and (99m) Tc: A phantom study. The Journal of Nuclear Medicine. 2000;41(8):14